

Article

Influence of Seawater Erosion on The Strength and Pore Structure of Cement Soil with Ferronickel Slag Powder

Feng Chen ^{1,2}, Shenghao Tong ^{3,*} , Hao Wang ²  and Weizhen Chen ²¹ College of Engineering, Fujian Jiangxia University, Fuzhou 350108, China² Zijin College of Geology and Mining, Fuzhou University, Fuzhou 350108, China³ College of Civil Engineering, Fuzhou University, Fuzhou 350108, China

* Correspondence: 210510001@fzu.edu.cn

Abstract: To promote the recycling of industrial waste residues in the reinforcement of foundation soil, the anti-seawater erosion of cement soil with ferronickel slag powder in the marine environment was studied. Specifically, this paper employed ferronickel slag powder to partially replace the cement. Then, the apparent morphology, unconfined compressive strength, and nuclear magnetic resonance (NMR) tests were performed on specimens of cement soil with ferronickel slag powder soaked in purified water and seawater. The research results reveal that with the rise in the content of ferronickel slag powder, the erosive effect of seawater on cement soil weakens, while the compressive strength of cement soil increases first and then decreases. With an excessive amount of ferronickel slag powder added to the cement soil, its chemically active effect decreases, leading to a decrease in the strength of the cement soil. When the admixture of ferronickel slag powder in cement soil is 45%, it achieves good performance. The addition of ferronickel slag powder improves the plasticity of cement soil. The higher the content of ferronickel slag powder, the greater the failure strain and residual strength of the cement soil. Microscopic studies indicate that with the increase in the content of ferronickel slag powder, the pores in the cement soil become smaller and smaller, the total pore volume decreases, the continuity of the pore size distribution improves, and the structure becomes more compact, thus enhancing the erosion resistance of cement soil.

Keywords: seawater environment; ferronickel slag powder; cement soil; erosion resistance



Citation: Chen, F.; Tong, S.; Wang, H.; Chen, W. Influence of Seawater Erosion on The Strength and Pore Structure of Cement Soil with Ferronickel Slag Powder. *Coatings* **2023**, *13*, 100. <https://doi.org/10.3390/coatings13010100>

Academic Editor: Andrea Nobili

Received: 29 November 2022

Revised: 27 December 2022

Accepted: 3 January 2023

Published: 5 January 2023



Copyright: © 2023 by the authors. Licensee MDPI, Basel, Switzerland. This article is an open access article distributed under the terms and conditions of the Creative Commons Attribution (CC BY) license (<https://creativecommons.org/licenses/by/4.0/>).

1. Introduction

Cement soil is widely used in road engineering, water conservancy, and construction projects because of its easy access to materials, good impermeability, great mechanical strength, and superior durability [1–4]. In recent years, more and more scholars have studied the mechanical properties of cement soil [5–8]. In order to meet engineering construction needs, the application environment of cement soil is also increasingly complex. Therefore, the mechanical properties of cement soil under a corrosive environment have gradually attracted widespread attention. Xiong et al. [9] and Chen et al. [10] studied the reactions between Cl^- , Mg^{2+} , SO_4^{2-} , and hydration products by conducting the unconfined compressive strength test and scanning electron microscope (SEM) and other microscopic tests. They found that the ion content degrades the strength of the cement soil, and that the coexistence of various corrosive ions has a greater impact on cement soil than a single type of ion. Xing et al. [11–13] immersed cement soil in erosion solutions with different ions to examine the impact of each ion on the strength of the cement soil. It was found that SO_4^{2-} , Mg^{2+} , and Cl^- affect the strength of cement soil at different stages. Specifically, SO_4^{2-} mainly participates in the early stage of the cement hydration reaction, Mg^{2+} mainly participates in the later stage of the cement hydration reaction, while Cl^- participates in the entire process of the cement hydration reaction. Mardani et al. [14] explored the influences of sulfate erosion and freeze–thawing on the permeability of kaolin reinforced by cement. They speculated

that sulfate erosion reduces the freeze–thaw resistance of cement–stabilized clay and that the freeze–thaw resistance of specimens using sulfate–resistant cement is better than that of ordinary Portland cement. Pham et al. [15] studied the destructive effect of sulfate on cement soil piles in the marine environment and found that the erosive effect of the marine environment on the soil–cement weakens the strength and deteriorates the mechanical properties of soil–cement piles. Li and Mousavi et al. [16,17] used ultrafine silica fume to partially replace cement and studied the mechanical properties of cement–solidified soil. They concluded that the unconfined compressive strength of cement–solidified soil increases with the rise in the content of ultrafine silica fume; Mangat et al. [18] studied the content of mineral residue and proposed that if the content of mineral residue is above 65%, the cement–based materials’ resistance to sulfate erosion can be improved. If the mineral residue content is below 65%, their resistance to sulfate erosion depends largely on the Al_2O_3 content. If the mineral residue content is lower than 50% and the Al_2O_3 content exceeds 18%, the mineral residue attenuates the erosion resistance. On the contrary, if the content of Al_2O_3 is lower than 11%, the mineral residue improves the erosion resistance. Aukkade Rerkpiboon et al. [19] used bagasse to partially replace ordinary Portland cement to increase its strength by 50%, while Eloy Asensio de Lucus et al. [20] proposed and discussed the use of clay–based construction and demolition waste (C&DW) as the pozzolanic additive. The results indicated that the addition of C&DW could significantly improve the durability and erosion resistance of cement.

In this study, composite ferronickel slag powder is used as the mineral admixture of cement soil. It is mixed into cement soil as a means of replacing cement with equal quality. The cement soil in a clean water environment is set as the control group, and the seawater environment is set as the test group. The cement soil surface morphology, unconfined compressive strength test, and nuclear magnetic resonance test are carried out. The corrosion resistance of ferronickel slag cement soil in a marine environment is investigated by combining macro and micro test methods.

2. Test Plan

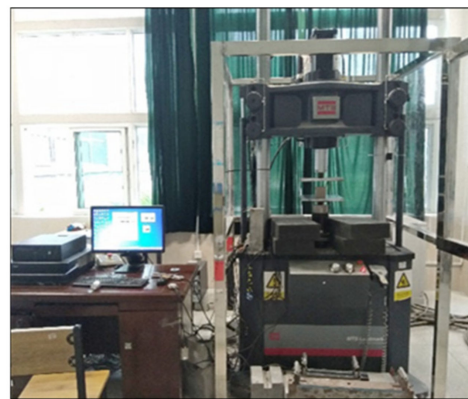
The soil used in the test was taken from the silt in the foundation pit of a project, with a moisture content of 58.6% and a plasticity index of 19.8. All water used was purified water. The cement used was ordinary Portland cement (P.O. 42.5). The formulation of the ferronickel slag powder was improved based on previous studies on the properties of ferronickel slag powder [21,22]. A certain amount of electric furnace ore powder was added to the formulation, thus formulating a new nickel–iron slag powder composite.

Three influencing factors were set up in the tests: the amount of ferronickel slag powder, soaking environment, and curing age. The mix proportions of the composite ferronickel slag powder in the cement soil were 0%, 10%, 20%, 30%, 45%, 50%, and 60%, respectively. The cement soil was demolded after being maintained in a standard maintenance box for 48 h. The demolded cement soil was placed in two immersion environments, water and seawater, for 7d and 28d, respectively. The cement soil with 0%, 10%, 20%, 30%, 45%, 50%, and 60% of composite ferronickel slag powder soaked in the purified water and seawater was coded as A–0, A–10, A–20, A–30, A–45, A–50, A–60, and B–0, B–10, B–20, B–30, B–45, B–50, B–60, respectively, as shown in Table 1. Three specimens were prepared for each numbered cement soil sample.

To measure the erosion resistance coefficient K_T , the evaluation index for the immersion erosion resistance of cement in Test Methods for Resistance of Concrete to Sulfate Erosion (GB/T 749–2008), the lateral limitless compressive strength test was carried out, and a standard test block of 70.7 mm × 70.7 mm × 70.7 mm was used. The unconfined test adopted the MTS landmark 370.25 (MTS, INC., Eden Prairie, MN, USA) testing machine (as shown in Figure 1) with a loading speed of 100 N/s. The test was carried out and the data processed according to the specific requirements in the Design Regulations for the Mix Proportion of Cement soil (JGJT233–2011).

Table 1. Preparation scheme of cement soil.

No.	Cement (%)	Water Cement Ratio	Compound Admixture Addition (%)	Environment
A-0			0	Purified water
A-10			10	
A-20			20	
A-30			30	
A-4			45	
A-50			50	
A-60	15	0.5	60	Seawater
B-0			0	
B-10			10	
B-20			20	
B-30			30	
B-45			45	
B-50			50	
B-60			60	

**Figure 1.** MTS landmark 370.25 testing machine.

Four ferronickel slag powder blending ratios of 0%, 30%, 45%, and 60% were designed for the NMR test. The tests were performed with a MesoMR12-060H-I NMR analysis and imaging system manufactured by Suzhou Newmark Analytical Instruments Co., Ltd. in Suzhou, China. The NMR instrument mainly consists of the permanent magnet, specimen tube, RF system, and data acquisition and analysis system. The cement soil specimen is a cylinder with a diameter of 50 mm and a height of 50 mm, as shown in Figure 2.

**Figure 2.** NMR test piece.

The erosion resistance coefficient of cement soil is calculated by Equation (1), and the strength depreciation rate is calculated by Equation (2) [10].

$$K_T = \frac{f_{u,s}}{f_{u,c}} \quad (1)$$

where K_T denotes the erosion resistance coefficient of the cement soil, accurate to 0.001; T denotes the soaking time in the water; $f_{u,s}$ denotes the compressive strength in seawater at time T ; and $f_{u,c}$ denotes the compressive strength in clean water at time T .

$$N_T = 1 - K_T \quad (2)$$

where N_T denotes the strength loss rate of the cement soil, accurate to 0.001.

The NMR transverse relaxation time T_2 is calculated based on Equation (3) through data inversion [23].

$$\frac{1}{T_2} = \rho_2 \frac{S}{V} \approx \rho_2 \frac{3}{R} \quad (3)$$

where T_2 denotes the transverse relaxation time; ρ_2 denotes the transverse relaxation rate; S/V —denotes the ratio of pore surface area to volume; and R —denotes the pore radius.

3. Test Results and Analysis

3.1. Apparent Erosion

After the cement soil with ferronickel slag powder is cured in purified water and seawater, the surface of the cement soil will undergo different changes. The 28-days-old cement soil cured in a purified water environment is shown in Figure 3, and the cement soil cured in a seawater environment is shown in Figure 4.

The cement soil with ferronickel slag powder (specimen in Group A) cured in purified water has a smooth surface, good integrity, and stable apparent characteristics (as shown in Figure 3), while the cement soil with ferronickel slag powder (specimen in Group B) cured in seawater shows different degrees of erosion.

After soaking in seawater for 28 days, the white substances on the surface of the specimen in B-0 coagulated into blocks. The cement soil soaked in seawater shows obvious erosion (as shown in Figure 4). The edges and corners of the specimen in B-30 were more comprehensive than those of the specimen in B-20. The integrity of the surface of the specimen in B-50 did not change significantly. It can be seen that with the increase in the content of ferronickel slag powder, the white crystalline substances on the surface of the cement soil become less and less, and the agglomerated blocks gradually become thin. This indicates that the addition of ferronickel slag powder into cement soil is beneficial to resist seawater erosion.

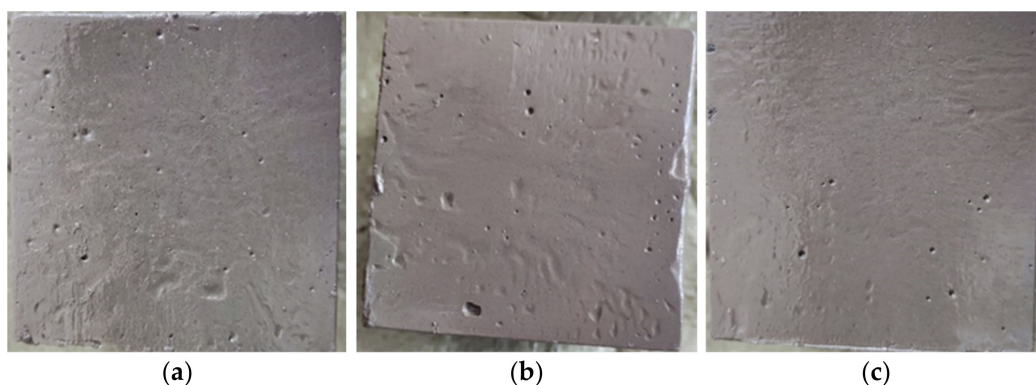


Figure 3. Apparent erosion image of cement soil soaked in purified water for 28 days. (a) A-0; (b) A-30; (c) A-50.

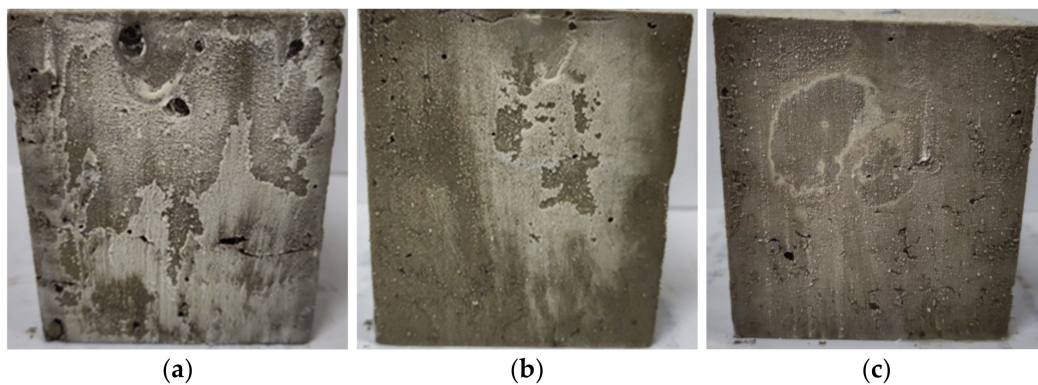


Figure 4. Apparent erosion image of cement soil soaked in seawater for 28 days. (a) B–0; (b) B–30; (c) B–50.

3.2. Influence of the Content of Ferronickel Slag Powder on the Compressive Strength of Cement Soil

The relationship between the unconfined compressive strength of the cement soil with ferronickel slag powder soaked for 7 days and 28 days and the content change of ferronickel slag powder is shown in Figure 5. The specific analysis of the influence of the content of ferronickel slag powder on the compressive strength of the cement soil is as follows.

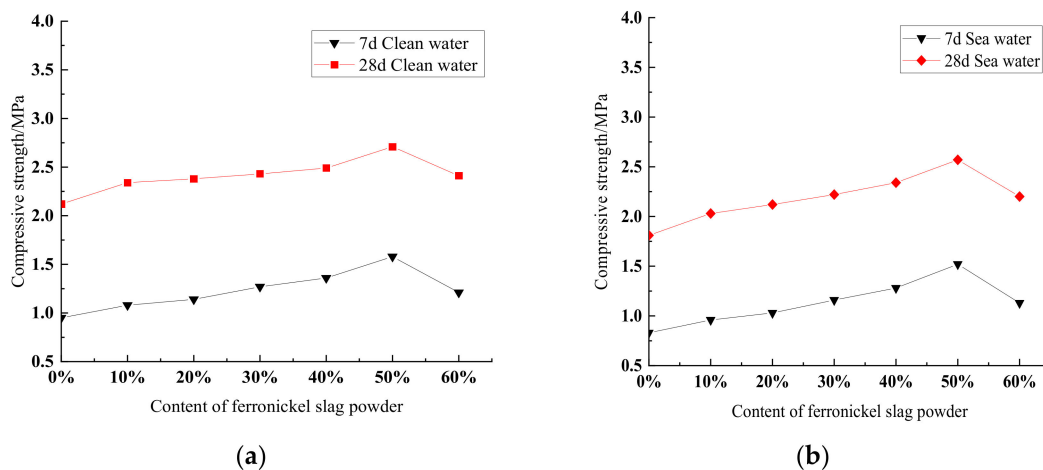


Figure 5. Relationship between the compressive strength of cement soil and the content of ferronickel slag powder. (a) Purified water environment; (b) seawater environment.

If the curing age is seven days, it can be seen from Figure 5 that the compressive strength curves of the cement soil soaked in purified water and seawater are basically the same. They show an inverted V-shaped trend with the increase in the content of ferronickel slag powder. The reason is that the curing age is short and the chemically active effect of the ferronickel slag powder is not fully developed. The excessive amount of ferronickel slag powder may result in the lack of reactants for the hydration reaction. When the content of ferronickel slag powder exceeds 50%, its compressive strength declines with the increase in content. According to the Technical Specifications for the Application of Mineral Residue in Cement Products (JC/T2238–2014), the applicable maximum limit of the quality of the cement replaced by the ferronickel slag powder is 45%, so the optimum content of the ferronickel slag powder in the cement soil is 45%. If the curing age is 28 days, it can be seen from Figure 5 that the compressive strength curves of the cement soil soaked in purified water and seawater are basically the same as those obtained in seven days. With the increase in the content of ferronickel slag powder, the compressive strength gradually increases, and it reaches the peak value when the content is 50%.

The sequential growth rates of the compressive strength of the cement soil soaked in purified water and seawater for 28 days are 10.38%, 1.71%, 2.10%, 2.47%, 8.84%, −11.07%, and 12.15%, 4.43%, 4.72%, 5.41%, 9.83%, −14.40%, respectively. Moreover, the sequential growth rate of A−10 and B−10 is the largest, indicating that the addition of ferronickel slag powder significantly improves the compressive strength of cement soil.

3.3. Influence of Marine Environment on Compressive Strength of Cement Soil

The relationship between the compressive strength of the cement soil with ferronickel slag powder soaked in purified water and seawater and the content change of ferronickel slag powder is shown in Figure 6. The erosion resistance coefficient K_T value and strength loss rate N_T of cement soil can be obtained by Equations (1) and (2). The results are shown in Tables 2 and 3.

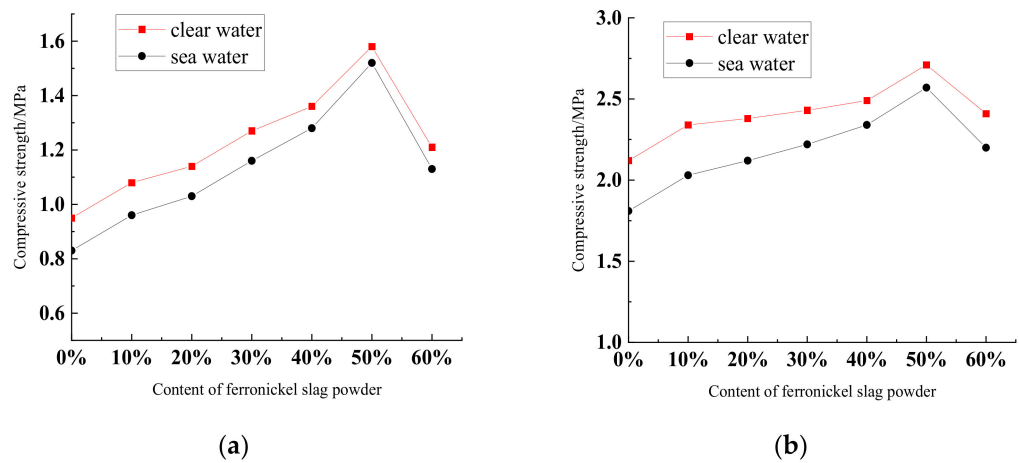


Figure 6. Compressive strength of cement soil with ferronickel slag powder soaked in purified water and seawater. (a) 7 d; (b) 28 d.

Table 2. Erosion resistance coefficient of cement soil with ferronickel slag powder.

Coefficient	Proportion						
	0%	10%	20%	30%	45%	50%	60%
K_7	0.875	0.892	0.905	0.911	0.943	0.966	0.934
K_{28}	0.852	0.868	0.891	0.914	0.940	0.948	0.913

Table 3. Strength loss rate of cement soil with ferronickel slag powder.

Loss Rate	Proportion						
	0%	10%	20%	30%	45%	50%	60%
N_7	12.8%	10.8%	9.5%	8.9%	5.7%	3.4%	6.6%
N_{28}	14.6%	13.2%	10.9%	8.6%	6.0%	5.2%	8.2%

As can be seen from Figure 6, the change trends of the strength curves of the cement soil soaked in purified water and seawater with a curing age of 7 days and 28 days are basically the same. With the increase in the content of ferronickel slag powder, the descending range of compressive strength of the cement soil soaked in seawater shows a decreasing trend. However, if the content of ferronickel slag powder exceeds 50%, the descending range becomes large.

As can be seen from Table 3, the N_7 and N_{28} values under different contents of ferronickel slag powder are 12.8%, 10.8%, 9.5%, 8.9%, 5.7%, 3.4%, 6.6%, and 14.6%, 13.2%, 10.9%, 8.6%, 6.0%, 5.2%, 8.2%, respectively. The strength loss rates N_7 and N_{28} show an inverted V-shaped trend with the increase in the content of ferronickel slag powder.

The N_7 and N_{28} values of the cement soil without ferronickel slag powder are 12.8% and 14.6%, respectively, obviously higher than those of other groups with the same curing age. However, the N_7 and N_{28} values of the cement soil with 50% of ferronickel slag powder are 12.8% and 14.6%, respectively, significantly lower than those of other groups with the same curing age. This reveals that the marine environment has an adverse effect on the strength of cement soil. The addition of ferronickel slag powder to cement soil not only improves the strength of the cement soil, but also helps resist seawater erosion. This is due to the fact that nickel–iron slag powder has a certain chemical activity, which is activated by 28 d of curing to produce hydration reaction products. These products fill the pores between the soil particles, making the cement soil more compact and preventing seawater from entering the cement soil, thus reducing the erosive effect of the seawater. However, excessive cement replacement by ferronickel slag powder is not conducive to resisting seawater erosion. In this case, it cannot activate ferronickel slag powder in the middle and late stages, causing an increase in hard–setting time and even the inability to shape the cement soil.

As can be seen from Table 2, the erosion coefficients K_{28} and K_7 under the same content of ferronickel slag powder are 0.852, 0.868, 0.891, 0.914, 0.940, 0.948, 0.913, and 0.875, 0.892, 0.905, 0.911, 0.943, 0.966, 0.934, respectively. K_{28} is lower than K_7 , except when the content is 30%. The seawater erosion enhances with the increase in the curing age. The influence of the marine environment on the strength of the cement soil with ferronickel slag powder is low under a curing age of 7 days. Under the same content of ferronickel slag powder, K_{28} is lower than K_7 . The erosive ions in seawater react with hydration products to form dilatants with low strength. These dilatants accumulate with the curing time, resulting in swelling stress and damage to the internal structure of the cement soil. Consequently, it reduces the strength and deteriorates the mechanical properties of the cement soil.

Figure 7 shows that the change trends of the stress–strain curves of the cement soil with different contents of ferronickel slag powder soaked in purified water and seawater are basically the same. The cement soil with ferronickel slag powder shows obvious brittle failure.

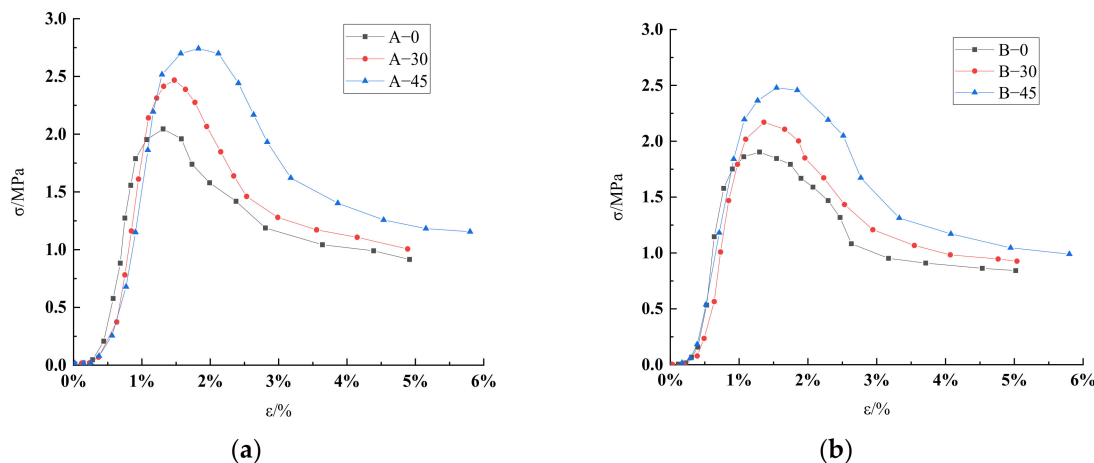


Figure 7. Stress–strain curve of cement soil with ferronickel slag powder. (a) Purified water environment; (b) seawater environment.

It can be seen from Figure 7 that under the same curing conditions, the failure strain of the cement soil increases continuously with the increase in the content of ferronickel slag powder. The failure strains of A–0, A–30, and A–45 in purified water are 1.32%, 1.55%, and 1.98%, respectively. The failure strains of B–0, B–30, and B–45 in seawater are 1.25%, 1.46%, and 1.81%, respectively. This indicates that the addition of ferronickel slag powder to cement soil can improve the plasticity of cement soil with ferronickel slag powder. After curing for 28 days, the ferronickel slag powder fills the pores in the cement soil as microaggregates, and undergoes a hydration reaction. The products are beneficial for improving the mechanical properties of cement soil. It also reveals that the residual

strength of stress–strain curves obtained under purified water and seawater environment increases with the rise in the content of ferronickel slag powder.

4. NMR Analysis of the Four–Pore Structure

The NMR images show the distribution of the number and size of the pores in the cement soil with ferronickel slag powder. As shown in Figures 8 and 9, with the increase in the content of ferronickel slag powder, the number of pixel points decreases, the color becomes lighter, and the distribution becomes uniform, indicating that the interior of the cement soil is dominated by small pores, with a homogeneous and dense state. However, if the content is 60%, the number of pixel points increases, with dense agglomeration and poor uniformity, indicating that the number of big pores increases and the porosity inside the cement soil increases. Compared to the cement soil with the same content of ferronickel slag powder in a purified water environment, the cement soil with ferronickel slag powder in a seawater environment has more pixel points, more obvious dense agglomeration, and worse uniformity. In Table 4, the porosity of B–0, B–30, B–45, and B–60 is 48.60%, 46.52%, 43.48%, and 45.56%, respectively, which is increased by 3.18%, 1.8%, 1.33%, and 0.81% compared to those under a purified water environment. The difference in the porosity between the two gradually decreases, and the seawater erosion gradually decreases, indicating that the addition of ferronickel slag powder into the cement soil weakens the erosive effect of seawater and enhances the compactness of the cement soil.

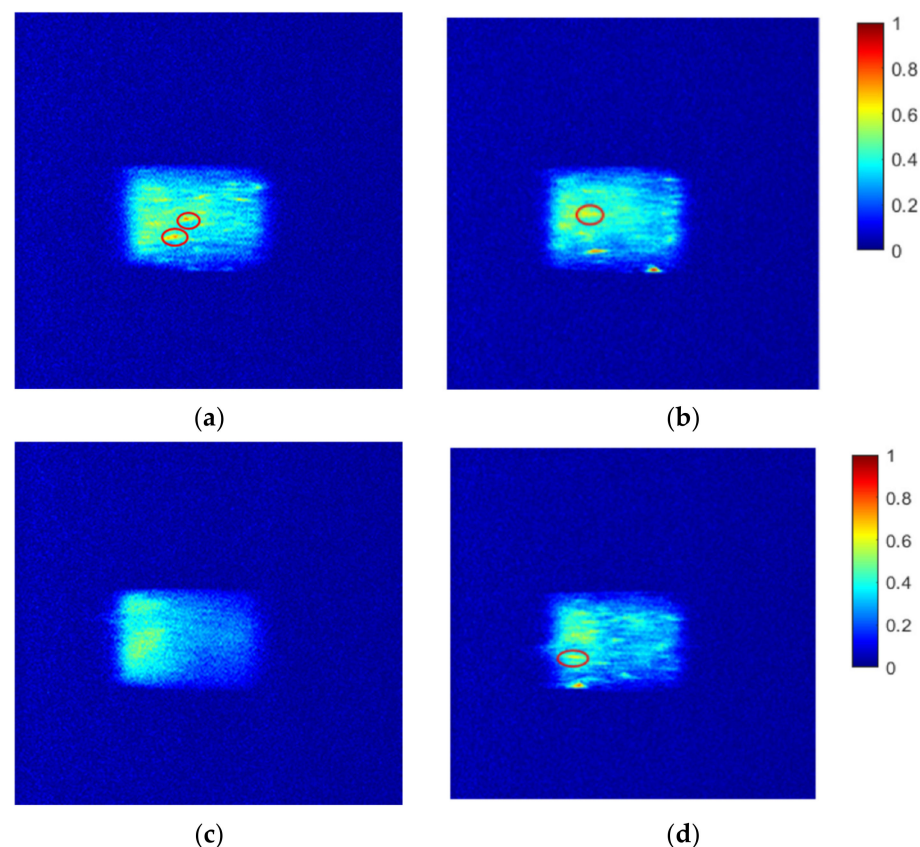


Figure 8. NMR pseudo–color image of cement soil with ferronickel slag powder under purified water environment. (a) A–0; (b) A–30; (c) A–45; (d) A–60.

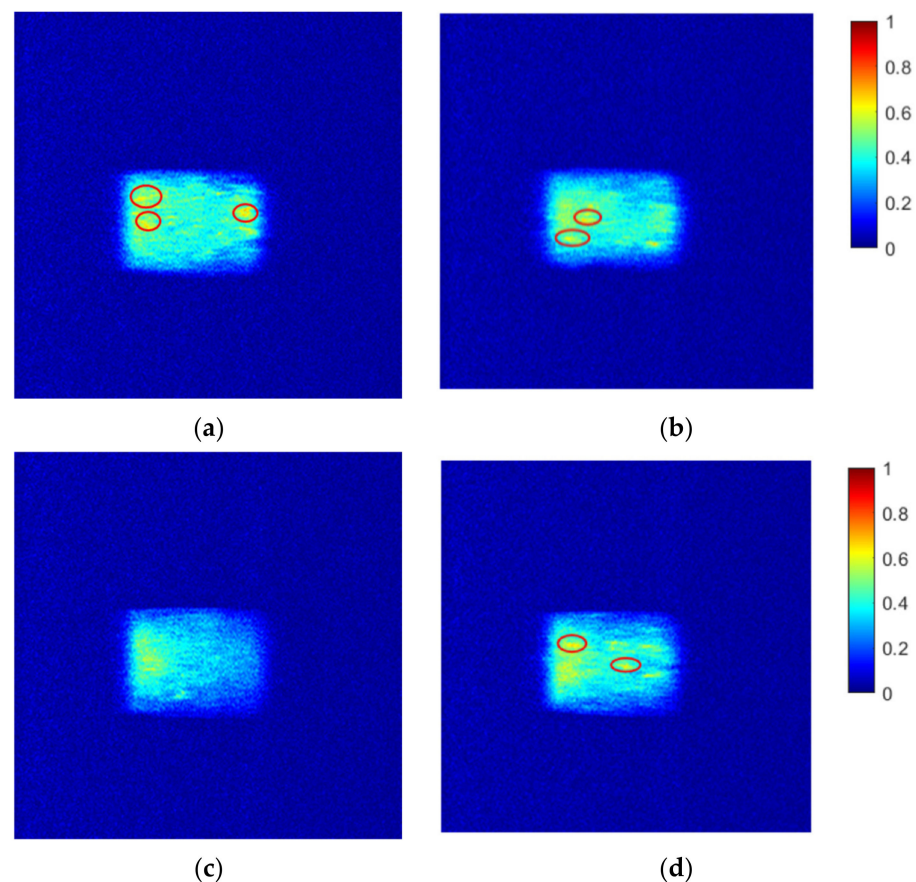


Figure 9. NMR pseudo-color image of cement soil with ferronickel slag powder under seawater environment. (a) B-0; (b) B-30; (c) B-45; (d) B-60.

Table 4. Porosity of of cement soil with ferronickel slag powder.

No.	A-0	A-30	A-45	A-60	B-0	B-30	B-45	B-60
Porosity/%	45.42	44.72	42.15	46.02	48.60	46.52	43.48	46.83

It can be seen from Table 4 and Figure 10a that with the increase in the content of ferronickel slag powder, the integrated peak area gradually decreases, indicating that the number of pores and the total pore volume decreases. When the initial value of T_2 gradually moves to the left, the terminal value of T_2 does not change significantly, and the peak signal amplitude gradually decreases, indicating the transformation of large pores into small ones, with the increase of small pores and the decrease of large ones. As shown in Figure 10b, the T_2 distribution curves of B-0 and B-30 show a bimodal pattern. The peak amplitude and integrated peak area of the P_2 of B-30 are smaller than those of the P_2 of B-0. B-45 and B-60 show unimodal distribution. As can be seen from Table 4, the peak T_2 values of B-0, B-30, and B-45 are 1.32 ms, 1.15 ms, and 0.96 ms, respectively, and the changing trend is consistent with that under a purified water environment. With the same content of ferronickel slag powder, the T_2 values increase by 0.12 ms, 0.07 ms, and 0.11 ms, respectively, compared with those under a purified water environment. Moreover, with the same content of ferronickel slag powder, the integrated peak areas of B-0, B-30, and B-45 are 45071, 44907, and 44114, respectively, and the T_2 values increased by 395, 1152, and 1203, respectively, compared with those under a purified water environment. This indicates that seawater erosion increases the number of pores, enlarges the pore size and the total pore volume, and decreases the compactness and integrity of the cement soil, resulting in the lower strength of the cement soil.

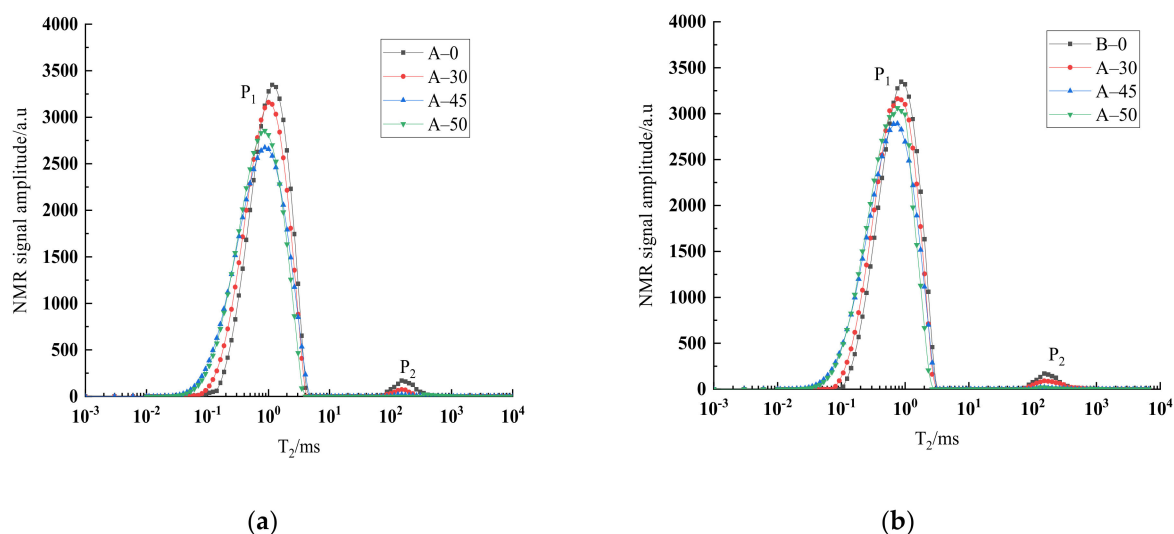


Figure 10. T_2 distribution curve of cement soil with ferronickel slag powder. (a) Purified water environment; (b) seawater environment.

5. Conclusions

(1) It can be seen from the apparent erosion characteristics that the surface of the cement soil cured in seawater suffers from erosion, and the edges and corners are passivated and fall off. The increase in the content of ferronickel slag powder makes the surface of the cement soil more complete and weakens erosion.

(2) The compressive strength of the cement soil can be improved by incorporating nickel–iron slag powder, and its compressive strength increases and then decreases with the amount of incorporation, and the maximum compressive strength is achieved at 50% of incorporation. The marine environment can deteriorate the strength of the cement soil; however, the incorporation of nickel–iron slag powder into the cement soil can resist the erosion effect of seawater, and the best effect is achieved at 45%.

(3) The ferronickel slag powder cement soil in the clear water environment and seawater environment shows brittle damage. The mixing of cement soil with nickel–iron slag powder enhances the plasticity of the cement soil, and the damage strain and residual strength increase with the increase in the mixing amount.

(4) The NMR test revealed that ferronickel slag powder can exert microaggregate effects in the cement soil. With the increase in the nickel–iron slag powder admixture, the large pores inside the cement soil decrease, the small pores increase, and the continuity of the pore size distribution becomes better and better. The total volume of the pores decreases and the structure is more dense.

Author Contributions: Conceptualization, F.C.; methodology, F.C. and S.T.; software, W.C.; validation, F.C., S.T. and W.C.; formal analysis, F.C.; investigation, S.T.; resources, F.C.; data curation, W.C.; writing—original draft preparation, F.C.; writing—review and editing, S.T.; visualization, W.C.; supervision, H.W.; project administration, H.W.; funding acquisition, F.C. All authors have read and agreed to the published version of the manuscript.

Funding: This research was funded by the Fujian University Industry University Research Joint Innovation Project (Grant No. 2022Y4002), the Natural Science Foundation of Fujian Province (Grant No. 2022J01963), and the Innovation Team Support Program of Fujian Jiangxia University.

Institutional Review Board Statement: Not applicable.

Informed Consent Statement: Not applicable.

Data Availability Statement: Not applicable.

Conflicts of Interest: The authors declare no conflict of interest.

References

1. Srijaroen, C.; Hoy, M.; Horpibulsuk, S.; Rachan, R.; Arulrajah, A. Soil-Cement Screw Pile: Alternative Pile for Low- and Medium-Rise Buildings in Soft Bangkok Clay. *J. Constr. Eng. Manag.* **2021**, *147*, 04020173. [[CrossRef](#)]
2. Santos Nascimento, E.S.; Souza, P.C.D.; Oliveira, H.A.D.; Melo Júnior, C.M.; Oliveira Almeida, V.G.D.; Melo, F.M.C.D. Soil-cement brick with granite cutting residue reuse. *J. Clean. Prod.* **2021**, *321*, 129002. [[CrossRef](#)]
3. Chen, F.; Tong, S. Experimental study on the strength of soil-cement with additions of mineral powder and ferronickel slag powder. *Int. J. Min. Miner. Eng.* **2020**, *11*, 218–227. [[CrossRef](#)]
4. Chen, F.; Tong, S. Impermeability Characteristics of Treated Marine Soft Soil with Ferronickel Slag Powder. *Geofluids* **2022**, *2022*, 1–10. [[CrossRef](#)]
5. Taslimi Paein Afrakoti, M.; Janalizadeh Choobasti, A.; Ghadakpour, M.; Soleimani Kutanaei, S. Investigation of the effect of the coal wastes on the mechanical properties of the cement-treated sandy soil. *Constr. Build. Mater.* **2020**, *239*, 117848. [[CrossRef](#)]
6. Manita, D.; Ashim, K.D. Use of Soil–Cement Bed to Improve Bearing Capacity of Stone Columns. *Int. J. Geomech.* **2020**, *20*, 6020008.
7. Cao, B.; Zhang, Y.; Xu, J.; Al-Tabbaa, A. Use of superabsorbent polymer in soil-cement subsurface barriers for enhanced heavy metal sorption and self-healing. *Sci. Total Environ.* **2022**, *831*, 154708. [[CrossRef](#)]
8. Sun, Y.; Cheng, J.; Li, Y.; Chen, Q.; Zhang, W.; Shao, G. Model test of the combined subgrade treatment by hydraulic sand fills and soil-cement mixing piles. *Bull. Eng. Geol. Environ.* **2020**, *79*, 2907–2918. [[CrossRef](#)]
9. Xiong, F.; Xing, H.; Li, H. Experimental study on the effects of multiple corrosive ion coexistence on soil-cement characteristics. *Soils Found.* **2019**, *59*, 398–406. [[CrossRef](#)]
10. Chen, F.; Tong, S. Effect of Ferronickel Slag Powder on Strength of Soil in Marine Environment. *Adv. Civ. Eng.* **2020**, *2020*, 1–10. [[CrossRef](#)]
11. Xing, H.; Yang, X.; Xu, C.; Ye, G. Strength characteristics and mechanisms of salt-rich soil–cement. *Eng. Geol.* **2009**, *103*, 33–38. [[CrossRef](#)]
12. Zhang, H.; Xing, H.-F.; Li, H.-M. Mechanical characteristic and microstructure of salt-rich cement soil. *Bull. Eng. Geol. Environ.* **2022**, *81*, 1–12. [[CrossRef](#)]
13. Haofeng, X.; Feng, X.; Feng, Z.; Wang, D.; Wiltshire, J. Improvement for the strength of salt-rich soft soil reinforced by cement. *Mar. Georesources Geotechnol.* **2018**, *36*, 38–42. [[CrossRef](#)]
14. Mardani-Aghabaglou, A.; Kalıpcılar, I.; İnan Sezer, G.; Sezer, A.; Altun, S. Freeze-thaw resistance and chloride-ion penetration of cement-stabilized clay exposed to sulfate attack. *Appl. Clay Sci.* **2015**, *115*, 179–188. [[CrossRef](#)]
15. Pham, V.N.; Turner, B.; Huang, J.; Kelly, R. Long-term strength of soil-cement columns in coastal areas. *Soils Found.* **2017**, *57*, 645–654. [[CrossRef](#)]
16. Li, Q.; Chen, J.; Shi, Q.; Zhao, S. Macroscopic and Microscopic Mechanisms of Cement-Stabilized Soft Clay Mixed with Seawater by Adding Ultrafine Silica Fume. *Adv. Mater. Sci. Eng.* **2014**, *2014*, 1–12. [[CrossRef](#)]
17. Mousavi, S.E. Utilization of Silica Fume to Maximize the Filler and Pozzolanic Effects of Stabilized Soil with Cement. *Geotech. Geol. Eng.* **2018**, *36*, 77–87. [[CrossRef](#)]
18. Mangat, P.S.; Khatib, J.M. Influence of Fly Ash, Silica Fume, and Slag on Sulfate Resistance of Concrete. *Mater. J.* **1993**, *2*, 542–552.
19. Rerkpiboon, A.; Tangchirapat, W.; Jaturapitakkul, C. Strength, chloride resistance, and expansion of concretes containing ground bagasse ash. *Constr. Build. Mater.* **2015**, *101*, 983–989. [[CrossRef](#)]
20. Asensio De Lucas, E.; Medina, C.; Frías, M.; Sánchez De Rojas, M.I. Clay-based construction and demolition waste as a pozzolanic addition in blended cements. Effect on sulfate resistance. *Constr. Build. Mater.* **2016**, *127*, 950–958. [[CrossRef](#)]
21. Chen, F.; Tong, S. Study on strength degradation of soil-cement mixed with composite ferronickel slag powder in marine environment. *J. Hydroelectr. Eng.* **2020**, *39*, 102–109.
22. Chen, F.; Tong, S.; Hao, W.; Shen, S. Dynamic Compression Properties of Ni-Fe Slag Powder Soil Cement under Impact Load. *Coatings* **2022**, *12*, 1003. [[CrossRef](#)]
23. Zhao, H.; Wu, X.; Huang, Y.; Zhang, P.; Tian, Q.; Liu, J. Investigation of moisture transport in cement-based materials using low-field nuclear magnetic resonance imaging. *Mag. Concr. Res.* **2021**, *73*, 252–270. [[CrossRef](#)]

Disclaimer/Publisher’s Note: The statements, opinions and data contained in all publications are solely those of the individual author(s) and contributor(s) and not of MDPI and/or the editor(s). MDPI and/or the editor(s) disclaim responsibility for any injury to people or property resulting from any ideas, methods, instructions or products referred to in the content.